

Soft Matter

Accepted Manuscript



This is an *Accepted Manuscript*, which has been through the Royal Society of Chemistry peer review process and has been accepted for publication.

Accepted Manuscripts are published online shortly after acceptance, before technical editing, formatting and proof reading. Using this free service, authors can make their results available to the community, in citable form, before we publish the edited article. We will replace this *Accepted Manuscript* with the edited and formatted *Advance Article* as soon as it is available.

You can find more information about *Accepted Manuscripts* in the [Information for Authors](#).

Please note that technical editing may introduce minor changes to the text and/or graphics, which may alter content. The journal's standard [Terms & Conditions](#) and the [Ethical guidelines](#) still apply. In no event shall the Royal Society of Chemistry be held responsible for any errors or omissions in this *Accepted Manuscript* or any consequences arising from the use of any information it contains.

Solvent-driven temperature memory and multiple shape memory effects

Rui Xiao^{1‡}, Jingkai Guo¹, David L. Safranski², Thao D. Nguyen^{1,3‡}

Thermally-activated temperature memory and multiple shape memory effects have been observed in amorphous polymers with a broad glass transition. In this work, we demonstrate the same shape recovery behaviors can also be achieved through solvent absorption. We investigate the recovery behaviors of programmed Nafion membranes in various solvents and compare the solvent-driven and temperature-driven shape recovery response. The results show that the programming temperature and solvent type have a corresponding strong influence on the shape recovery behavior. Specifically, lower programming temperatures induce faster initial recovery rates and larger recovery, which is known as temperature memory effect. The temperature memory effect can be used to achieve multi-staged and multiple shape recovery of specimens programmed at different temperatures. Different solvents can also induce different shape recovery, analogous to the temperature memory effect, and can also provide a mechanism for multi-staged and multiple shape memory recovery.

1 Introduction

Shape memory polymers (SMPs) can memorize single or multiple temporary shapes and have the ability to recover to their permanent shapes in response to environmental stimulus, such as heat^{1–7}, light^{8–11}, pH¹² or solvent^{13–21}. Among all of the different types of SMPs, temperature-activated amorphous SMPs are the most extensively investigated because of the variety of polymer types, simplicity in synthesis, availability of characterization methods and constitutive models^{22–26,28–34}. The solvent-driven shape memory effect (SME) provides an alternative athermal activation method for amorphous polymers. Solvent-driven shape recovery is attractive for biomedical applications^{35–37}, such as implantable medical devices (stents, heart valves) and drug delivery capsules, because of the difficulty in heating the device in a surgical procedure. Solvent-driven shape recovery can also be applied to industrial areas, such as for sand-control screens in petroleum engineering³⁸, where the fluid environment provides a good medium for driving shape memory recovery. Though the two activation methods appear different, they share the same physical mechanism for amorphous polymers. The SME is achieved through deploying the programmed SMPs at the temperature above the transition temperature either by increasing the ambient temperature (temperature-activated mechanism)^{4,39} or by decreasing the glass transition temperature (solvent-activated mechanism)^{13,40–42}. Thus, specific recovery behaviors achieved in temperature-driven shape recovery, such as temperature memory and multiple shape memory, may also be observed in solvent-driven recovery.

Temperature memory effect (TME) refers to the ability of amorphous SMPs to memorize the programming temperature^{43–54}. Specifically, for specimens programmed at lower temperatures, both the recovery region in the free recovery tests and the peak stress in the constrained recovery tests shifts to lower temperatures. TME provides a flexible method to tune the shape recovery behaviors without changing chemical composition of polymers. For polymers with a broad glass transition, the temperature memory effect can be exploited to achieve multiple shape memory recovery^{55–57}. Multiple temporary shapes can be programmed at different temperatures. During deployment, the specimens exhibit stepwise shape recovery when approaching the programming temperature of each temporary shape. In addition to the programming conditions, the recovery condition also has a significant

¹Department of Mechanical Engineering, Johns Hopkins University, Baltimore, MD, 21218.

²MedShape Inc, 1575 Northside Drive NW Suite 440, Atlanta, GA 30318, USA.

³Department of Materials Science and Engineering, Johns Hopkins University, Baltimore, MD, 21218.

[‡]Corresponding authors: rxiao4@jhu.edu (R. Xiao); vicky.nguyen@jhu.edu (T. D. Nguyen).

effect on the shape memory performance. For SMP materials programmed with only one temporary shape, the recovery behavior can be distributed into several quasi-equilibrium parts by deploying the SMPs at multiple discrete temperature steps. Both multiple and multi-staged shape memory behaviors have attracted great interest since they can significantly expand the potential applications of SMPs.

In this paper, we demonstrate the temperature memory and multiple shape memory effects can also be achieved by solvent-driven shape recovery. We first investigated the influence of deformation temperature and solvent type on the recovery behaviors of Nafion membranes with a single programmed temporary shape. The results indicate that the specimens programmed at a lower temperature exhibit a higher recovery rate and shape recovery. It is also observed different solvents exhibit different shape recovery abilities. We exploited these findings to achieve the multiple and multi-staged shape memory recovery behaviors. It is found that the programmed Nafion films showed stepwise shape recovery when programmed with two temporary shape at two different temperatures. The specimens exhibit staged recovery when immersed in multiple solvents. The residual unrecoverable strain in solvent can be further activated through heat, indicating solvents do not change the chemical structures of Nafion. For each set of shape recovery experiments in solvent, the corresponding temperature-activated experiments were performed to demonstrate the underlying mechanisms of the two activation methods are the same.

2 Experimental procedure

2.1 Materials

The SMP material used in this study was Nafion® PFSA membrane with equivalent molecular weight 1100 (Dupont, Wilmington, DE, USA) and was purchased from Ion Power (New Castle, DE, USA). The acetone ($\geq 99.8\%$), ethanol ($\geq 99.5\%$) and isopropyl alcohol ($\geq 99.5\%$) (IPA) were ordered from Sigma Aldrich and used as received. Prior to all the measurements, the specimens were annealed at 160°C for half a hour to remove the water in the specimens.

2.2 Swelling tests

Film specimens with dimension $4.0 \times 4.0 \times 0.25 \text{ mm}^3$ were used to measure the equilibrium swelling ratio. Each specimen was weighed before testing. The specimens were immersed in the solvent for one day and weighed using a digital balance with 10^{-4} gram resolution. The weight of the specimens with longer immersion time showed negligible change suggesting an equilibrium swelling ratio was achieved after one day. In order to measure the swelling rate, the film specimens were also removed periodically and weighed. The following solvents were chosen: acetone, ethanol, water, IPA, and mixture solutions of IPA and water with different mass ratio. For each measurement, four specimens were repeated. The swelling ratio S_w is defined as,

$$S_w = \frac{m_{eq} - m_0}{m_0} \quad (1)$$

where m_0 is the initial dry weight and m_{eq} is the equilibrium specimen weight.

2.3 Dynamic temperature sweep

The dynamic temperature sweep test was used to characterize the temperature dependent storage modulus and $\text{Tan } \delta$. The test was run under the dynamic mode of DMA at 1 Hz frequency with specimen size $12 \times 5 \times 0.25 \text{ mm}^3$. The specimen was equilibrated at 20°C for 20 minutes and then heated to 180°C at $1^\circ\text{C}/\text{minute}$ under 0.4% dynamic strain.

2.4 Shape recovery experiments

2.4.1 Programming temperature: Film specimens with size $12 \times 10 \times 0.25 \text{ mm}^3$ were used for the tests. Prior to the tests, a $5 \text{ mm} \times 5 \text{ mm}$ square marker was drawn on the specimen in the length and width direction. The specimens were equilibrated at 160°C , 140°C , 120°C , 100°C or 80°C for 15 minutes to reach heat conduction equilibrium before stretched to 60% engineering strain in 2 minutes. The specimens were then cooled to 20°C at $10^\circ\text{C}/\text{minute}$ with constant strain and held isothermally for 5 minutes before unloading. For recovery in solvent, the specimens were unmounted from DMA and immersed in solvents (acetone, ethanol, IPA and water mixture with mass ratio 1:9 and 5:5). For specimens programmed at 160°C or 140°C , pure IPA and IPA and water mixture with mass ratio 2:8 were also adopted as solvents. A digital camera was used to record the temporary shape every 6 seconds. For specimen recovery in air, the programmed specimens were heated to 130°C at $20^\circ\text{C}/\text{minute}$ and held for 30 minutes.

2.4.2 Dual programming shape recovery: Dual programming shape recovery tests were performed on cruciform specimens. The specimens were first stretched in one direction to 60% engineering strain at 160°C in 2 minutes and cooled to 20°C . The specimens were then mounted in the perpendicular direction and heated to 80°C and annealed for 10 minutes to allow the specimens to reach equilibrium length. The specimens were stretched an additional 60% engineering strain and cooled to 20°C . The specimens were then immersed in acetone or ethanol to measure the recovery behaviors.

2.4.3 Multi-staged shape recovery: The film specimens with size $12 \times 10 \times 0.25 \text{ mm}^3$ were stretched to 100% engineering strain at 160°C or 140°C . The specimens were then cooled to 20°C at $10^\circ\text{C}/\text{minute}$. During the recovery process, the specimens were subsequently immersed in an IPA and water mixture with mass ratio 1:9, 2:8 and 5:5 for 10 minutes in each solution. For shape recovery in air, the programmed specimens were heated in discrete steps at $20^\circ\text{C}/\text{minute}$. Three recovery temperatures were chosen: 100, 120 and 140°C . The specimens were held at each temperature for 30 minutes.

2.4.4 Temperature-driven shape recovery of specimens with or without solvent treatment: The thermally-activated shape memory tests were also performed on specimens with or without recovery in solvent. The specimens were stretched to 60% engineering strain at 160°C and cooled to 20°C to fix the temporary shape. For specimens without solvent treatment, the specimens were directly heated to 190°C at $1^\circ\text{C}/\text{minute}$ under zero force mode of DMA. For specimens with solvent treatment, the specimens were immersed in solvent (acetone, ethanol, IPA and water mixture with mass ratio 1:9 and 5:5) for 30 minutes. The specimens were then placed at 70°C in an incubator for 30 minutes to fully evaporate the solvents. The specimens were heated from 70°C to 190°C at $1^\circ\text{C}/\text{minute}$ under zero force mode of DMA.

3 Results

Nafion material investigated in this study exhibits a broad glass transition region from 40°C to 145°C as shown in Fig. 1. In our previous work⁵³, we demonstrated the temperature memory effect and multiple shape memory effect of this material through heat. In this work, we first investigated the recovery behaviors of a single programmed shape in solvent.

3.1 Single programming shape

The Nafion films were stretched to 60% engineering strain at different programming temperatures on a DMA Q800 and recovered in solvent at room temperature, as described in Section 2.4.1. Since Nafion shows large swelling abilities in the selected solvents, a square marker was drawn in the center of the specimen. The aspect ratio of the marker was defined as: $a = l(t)/w(t)$, where $l(t)$ and $w(t)$ are the length and width of the marker at time t . The stretch at time t caused by the mechanical deformation in the length direction is λ_m . By assuming the material is mechanically incompressible, the stretch in the width direction can be calculated as, $\lambda_m^{-1/2}$. We further assume the swelling behavior is isotropic, producing a stretch λ_s in each direction. Thus, the aspect ratio can be calculated as:

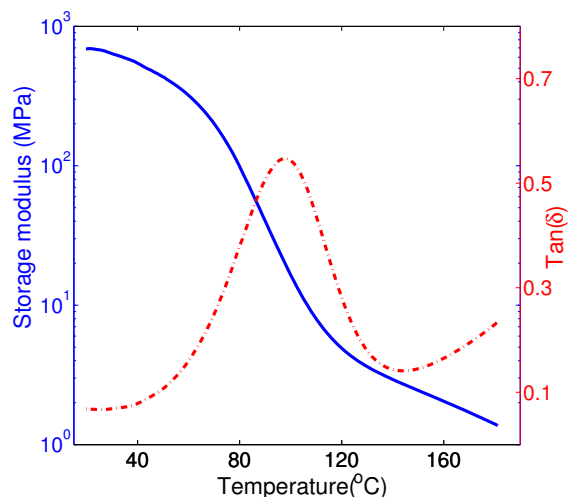


Fig. 1 The storage modulus and Tan δ of Nafion measured from the dynamic temperature sweep tests at 1 Hz frequency

$a = (\lambda_m \lambda_s) / (\lambda_m^{-1/2} \lambda_s) = \lambda_m^{3/2}$. In order to quantitatively compared with the thermally-activated shape recovery response, we then define the equivalent strain $\epsilon_e = a^{2/3} - 1$. Due to the influence of the clamp in the programming step, the strain in the specimens is inhomogeneous. Thus cautions should be taken when compared the equivalent strain with the strain measured from the DMA.

Fig. 2.a shows the recovery performance of programmed Nafion films in ethanol. The deformation temperature had a large influence on the recovery behavior. Specimens programmed at 80°C, 100°C and 120°C showed full recovery after immersing in ethanol for 10 minutes. Specimens programmed at 140°C and 160°C only showed partial recovery. The lower deformation temperature also resulted in a faster recovery rate. Specimens programmed at 80°C required only 60 seconds to achieve full recovery while almost 400 seconds was needed to reach full recovery for specimens programmed at 120°C. During the recovery process, the specimens did not exhibit buckling or wrinkling as observed in previous works^{19,21,58-60}, mainly because the specimens were thin (0.25 mm), which allowed for uniform swelling.

To compare the temperature-driven and solvent-driven activation mechanisms, the shape recovery tests were also performed by heating the specimens to 130°C at 20°C/minute in the DMA under zero force mode (Fig. 2.b). Both the temperature-driven and solvent-driven recovery responses show a similar increase in the unrecovered strain with the programming temperature.

In addition to ethanol, we performed shape recovery experiments in acetone, and a mixture of IPA and water. The temperature memory effect was observed for all the solvents investigated in this work (Fig. 3.a). Different solvents also produced different shape recovery. The largest shape recovery occurred in the 50%IPA-50%water solution (50%IPA), while the least occurred in the 10%IPA-90%water solution (10%IPA). The shape recovery experiments were also performed for other IPA concentrations (Fig. 3.b). The shape recovery first increased and then decreased with increasing IPA concentration. In order to understand this observation, we measured the equilibrium swelling ratio of the Nafion film in the different solvents as described in Section 2.2. As shown in Fig. 4, Nafion experienced minimal swelling in water, which was consistent with the result that the programmed specimen showed negligible recovery in water after 10 minutes (data not shown). The maximum swelling ratio was observed in 50%IPA solution. The shape recovery and swelling ratio in different solvents showed a similar trend.

Fig. 5 plots the normalized swelling ratio of Nafion in acetone, ethanol, 10%IPA and 50%IPA with time. The Nafion films achieved more than 60% equilibrium swelling ratio within 5 minutes in all cases, which explained

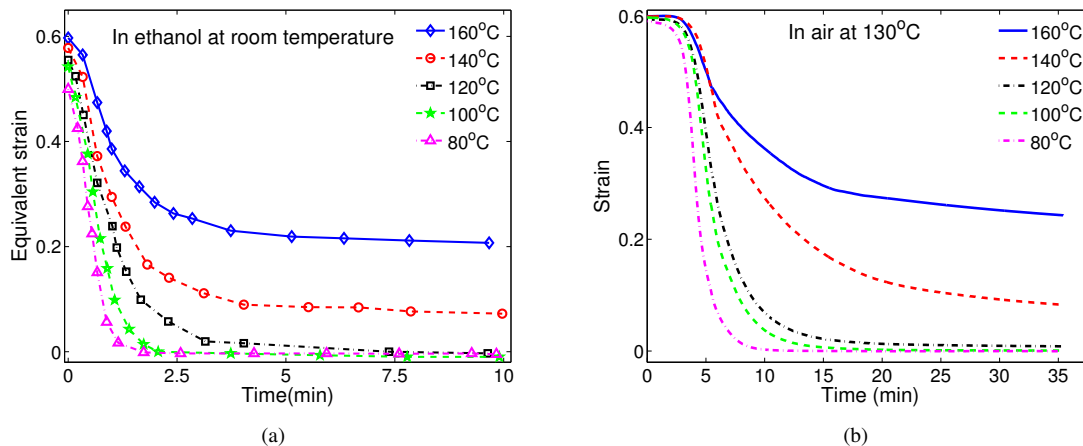


Fig. 2 Influence of programming temperature on the shape recovery of Nafion: a) in ethanol at room temperature b) in air at 130°C

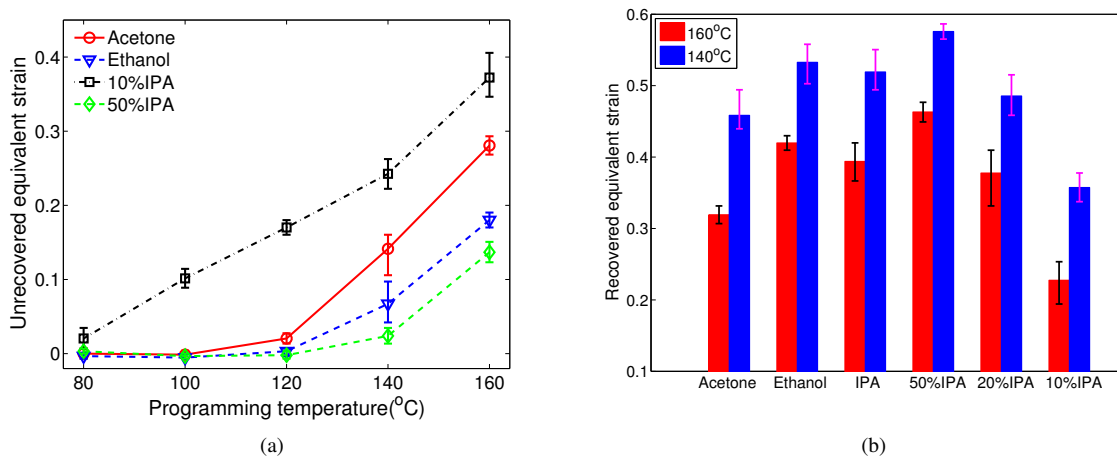


Fig. 3 Recovery performance of Nafion in solvents: (a) the unrecovered strain as a function of different programming temperatures, (b) the recovered strain of specimens programmed at 160°C and 140°C and recovered in different solvents.

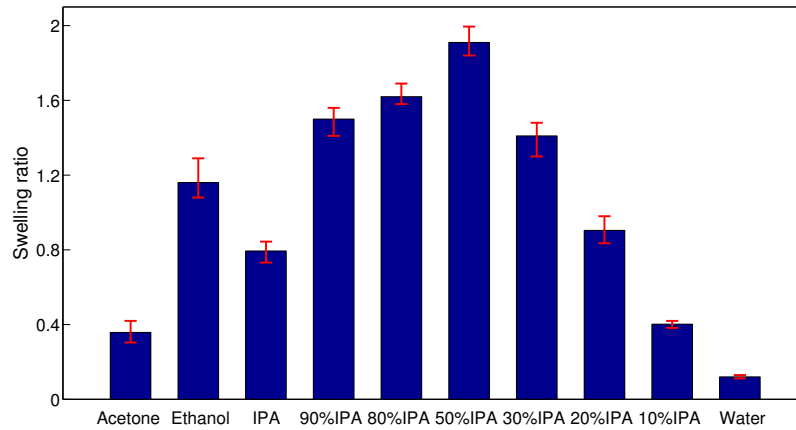


Fig. 4 Swelling ratio of Nafion in different solvents.

how the programmed specimens were able to attain a quasi-equilibrium recovered state after 5 minutes in solvent.

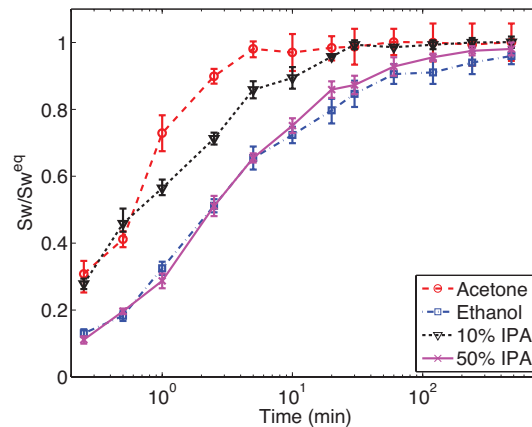


Fig. 5 Swelling rate of Nafion in different solvents.

3.2 Multiple and multi-staged shape recovery

The temperature memory effect can be employed to design multiple shape memory recovery in solvents. We first qualitatively demonstrates a triple shape memory recovery effect. Two temporary shapes were programmed at 160°C and 70°C. The specimen was first stretched to 100% engineering strain at 160°C and then curled at 70°C (Fig. 6). The specimen was then immersed in 10%IPA at room temperature for 10 minutes and then transferred into 50%IPA for another 10 minutes. The subsequent shape recovery is shown in Fig. 6. The shape programmed at 70°C achieved full recovery within 90 seconds in 10%IPA. The shape programmed at 160°C exhibited slight recovery after 10 minutes in 10%IPA. The shape further recovered in 50%IPA to nearly the original aspect ratio indicating different solvents exhibited different shape recovery abilities. For comparison, we performed the recov-

ery experiments by immersion in 50% IPA only. The specimen recovered significantly quicker in 50%IPA. The shape programmed at 70°C recovered fully after 18 seconds and the shape programmed at 160°C recovered almost fully after 600 seconds.

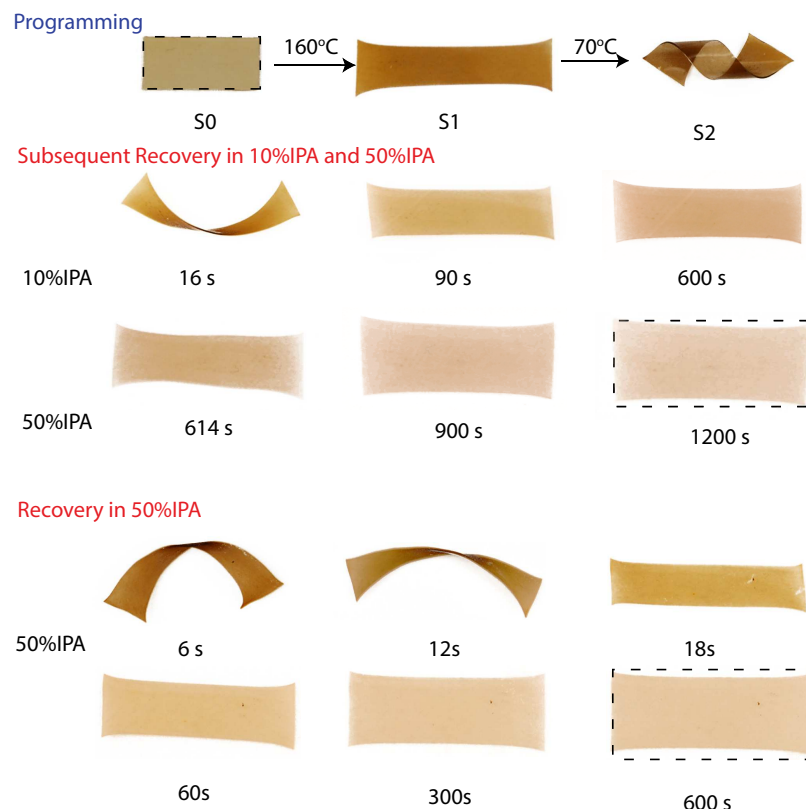


Fig. 6 The demonstration of shape recovery of Nafion films programmed with two temporary shapes at 160°C and 70°C, recovered sequentially in 10%IPA and 50%IPA, and recovered in 50%IPA .

To quantitatively measure the triple shape memory effect in solvent, specimens were stretched to 60% strain in the length direction at 160°C and an additional 60% strain in the width direction at 80°C, as described in Section 2.4.2. Fig. 7 shows a schematic of the programming process. Fig. 8 plots the equivalent strain of the specimens during the recovery in acetone or ethanol. As shown, the equivalent strain first increased indicating the recovery of the second programmed shape and then decreased to a steady state value which was caused by the recovery of the first programmed shape. The specimens in ethanol showed a larger recovery than in acetone, which is consistent with the experimental results in Fig. 3.

Multi-staged shape recovery can be achieved by sequential immersion of the programmed specimens in different solvents, as described in Section 2.4.3. Fig. 9.a plots the recovery performance for specimens programmed at 160°C or 140°C and recovered subsequently in 10%, 20% and 50%IPA. The specimens exhibited a three-staged shape recovery performance, one for each solvent solution. For comparison, we applied a series of temperature steps to deploy the programmed Nafion film. The specimen was heated to 100, 120, 140°C and held at each temperature for 30 minutes. The specimens reached the quasi-equilibrium state within the 10 minutes immersed in each solvent solution in Fig. 9.a, as well as during the 30 minutes at each temperature, 100, 120 and 140°C in Fig. 9.b.

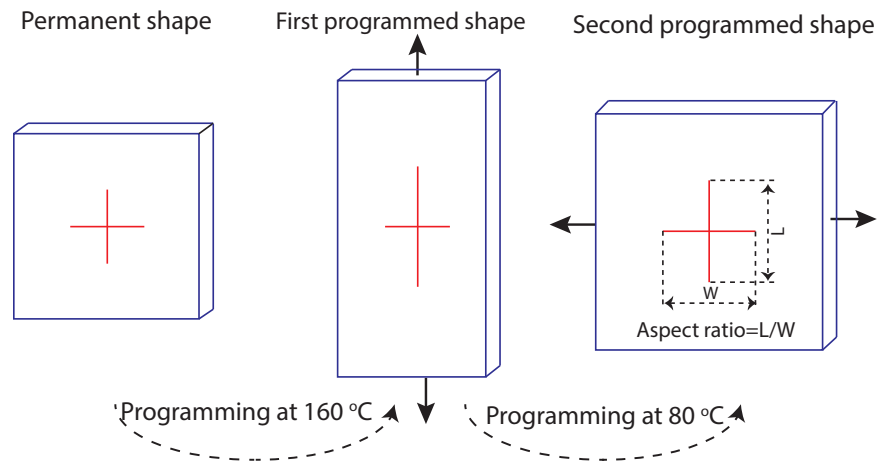


Fig. 7 The schematic of specimens programmed with two temporary shapes at 160°C and 80°C.

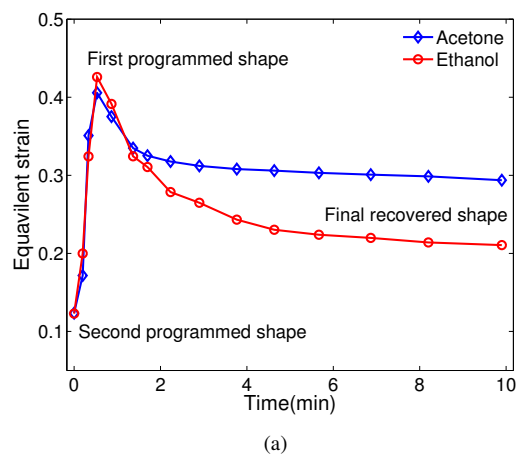


Fig. 8 The recovery performance of specimens programmed with two temporary shapes and recovered in acetone or ethanol.

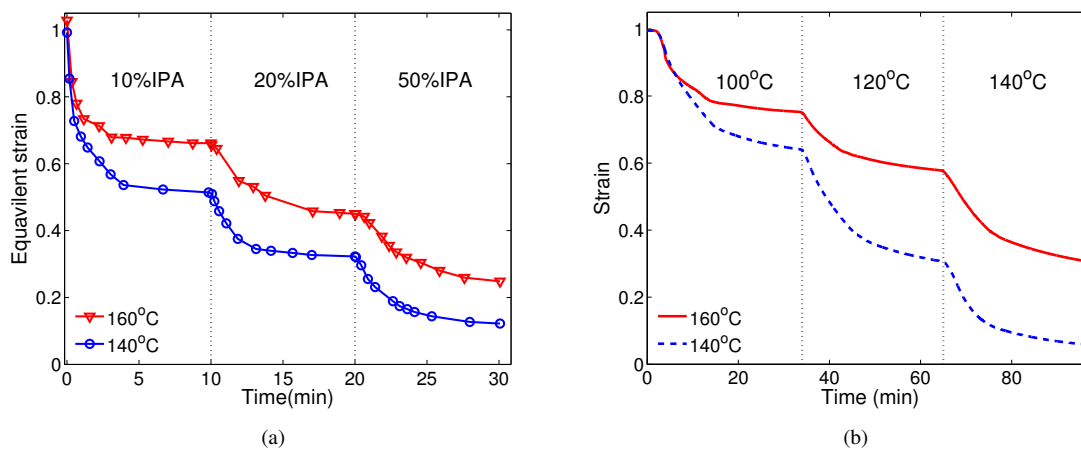


Fig. 9 Multi-staged shape recovery of specimens programmed at 160°C or 140°C and recovered: (a) in multiple solvents, (b) at multiple temperatures.

3.3 Combination of the solvent and heat to achieve shape recovery

As shown in Fig. 3, the specimens programmed at 160°C did not achieve full shape recovery in any of the solvents investigated in this work. We next investigated whether further shape recovery can be activated through heat. As shown in Fig. 10, the temperature-driven free recovery of specimens treated with different solvents had different activation temperatures, varying from 100°C for 10%IPA to 140°C for 50%IPA. However, all specimens fully recovered by 170°C and the recovery curves merged at higher temperatures. The different solvent treatments did not induce irreversible changes to the chemical and physical structure of the Nafion material. From this result, we can also see the possibility of tuning the temperature-driven shape recovery region through pretreatment in an appropriate solvent. The recovery region of the Nafion without solvent treatment shows a broad recovery region with 80°C-170°C, while the recovery region with 50%IPA treatment is narrowed to 140°C-170°C.

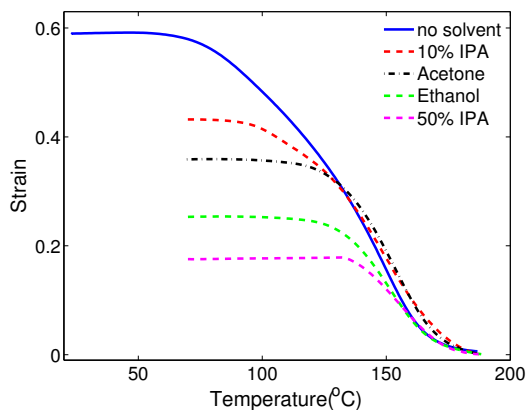


Fig. 10 The thermally activating the residual strain after recovery in solvent

4 Discussion and Conclusions

To quantitatively characterize the temperature memory effect, the deformation temperature is often related with the maximum strain recovery speed in the free recovery tests^{49,52} or the maximum recovery stress in the fixed-strain recovery tests^{61,62}. In our work, we employed the isothermal recovery conditions for both temperature-driven or solvent-driven mechanism. The deformation temperature was related with the unrecovered strain to define the temperature memory effect. The specimens programmed at higher temperatures showed less recovery and exhibited a larger unrecovered strain in both solvent-driven and temperature-driven mechanisms. The solvent-driven mechanism is analogous to the temperature-driven mechanism. The temperature-driven mechanism brings the temperature of the specimen above the activation temperature while the solvent-driven mechanism lowers the activation temperature to below the specimen temperature.

To understand the underlying mechanism behind the temperature memory and multiple shape effects, several models have been developed in recent years^{48,50,52,53}. These models considered Nafion as a viscoelastic material with a broad distribution of relaxation times. The large relaxation times are related to the rearrangement and rotation of larger segments of the polymer chain, and require high temperatures to activate. When deformed at a certain temperature, only the relaxation processes with relaxation times comparable or smaller than experimental time relax to equilibrium, while relaxation processes with a relaxation time significantly larger than the experimental time remain in the nonequilibrium state. The temporary shape deformed at a lower temperature is stored in relaxation processes with smaller relaxation times (smaller segments) and requires a lower activation temperature for shape recovery.

The multiple shape memory behavior is the result of programming multiple temporary shapes at different temperatures. The temporary shapes are stored in different relaxation processes with different relaxation times. Shapes programmed at lower temperatures are fixed by shorter relaxation times, and recover before shapes programmed at higher temperatures, which are fixed by longer relaxation times. The temperature memory effect can be observed in polymers with a relative narrow glass transition⁵². However, in order to achieve multiple shape memory effect, the recovery region of each temporary shape has to separate from each other which requires a broad glass transition.

The same mechanisms also produce the solvent-driven temperature memory and multiple shape memory effects. Nafion is composed of a tetrafluoroethylene backbone with perfluorovinyl ether with a terminal sulfonic acid group. The swelling behavior of Nafion in various solvents has been investigated experimentally and theoretically^{63–65}. Yeo⁶³ experimented with a number of polar solvents to relate the degree of swelling to the solubility parameter, the square root of the cohesive energy density. Two solubility parameters were reported for Nafion due to dual swelling envelopes, and it was suggested that one envelope existed for the backbone and the other for the ionic group. In contrast, Gebel *et al.*⁶⁵ expanded the range of solvents compared to Yeo⁶³, Yeo and Cheng⁶⁴, and found that the solubility parameter was not a good predictor of swelling behavior due to scattered data. Instead, the donor number of the solvent was determined to be a more accurate predictor of the swelling behavior, where a maximum in swelling existed between 25–30 kcal/mol. In this study, the swelling behavior displayed a maximum for 50%IPA, which is consistent with results in Gebel *et al.*⁶⁵ for mixtures of water and isopropanol.

The structure of the crystalline tetrafluoroethylene backbone and ionic sulfonic acid group of Nafion has been characterized by small angle neutron scattering with varying alcohols and water. Scattering maxima exist for the crystalline region and ionic region, and the Bragg spacing of these maxima increases as solvent levels increase. The alcohols were found to preferentially partition into the regions of the polymer other than the ionic region⁶⁶. A series of molecular dynamic simulations support this partition of alcohols to the crystalline tetrafluoroethylene regions when a water-alcohol mixture is present. This occurs because of the preference for van der Waals interactions between the CH_3 group of the alcohol and the tetrafluoroethylene backbone, while both water and alcohol participate in hydrogen bonding with the ionic group^{67,68}. In addition, the backbone mobility increased as the solvents mixed, where four conformational transitions were observed for water, seven for methanol, and twelve for a water-methanol mixture⁶⁸. This supports the results seen here where the 50%IPA mixture showed greater recovery than pure water or IPA due to the increased chain mobility of the tetrafluoroethylene backbone.

The absorption of solvents depresses the Tg of the polymer network by increasing the chain mobility. This decreases the relaxation time allowing for shape recovery. Previously, we have developed a model⁴¹ based on the Adam-Gibbs configurational entropy theory^{69–71} to explain the solvent-driven shape memory behaviors. In the classic theory of Adam-Gibbs⁶⁹, the relaxation time (viscosity) is inversely dependent on configurational entropy. When solvent diffuses into the polymer matrix, it increases the configurational entropy due to the mixture of solvent and polymer segments⁷¹. In this work, we found that different solvents produced different shape recovery. The solvent with the stronger swelling induced more shape recovery. This could be attributed to a larger increase in configurational entropy with a larger amount of solvents, resulting in a larger decrease in viscosity and relaxation time. The influence of solvent absorption on viscosity and relaxation time can be measured using the dynamic frequency sweep tests⁴¹ or differential scanning calorimetry tests¹³ on dry and saturated specimens. However, the swollen thin Nafion films dried in air after less than 2 minutes, and we would need to design DMA experiments for specimens fully immersed in solvent. This is a subject of future work.

Though shape memory polymers have been extensively investigated in recent years, they are still not widely used. One possible reason is the strong restriction of the activation condition which typically requires high temperatures. The solvent-driven mechanism provides an alternative mechanism which can induce shape recovery at lower temperatures and with energy saving. In this paper, we showed that solvent-driven mechanism exhibits the same key shape memory phenomena as temperature-driven mechanism. Specially, the solvent-driven mechanism also exhibits the temperature memory and multiple shape memory effects. We believe the same phenomena, such as multiple and multi-staged shape memory recovery, can also be observed for biopolymers in the human body. Thus, this work could potentially advance biomedical applications of shape memory polymers.

Acknowledgements

The authors gratefully acknowledge the funding support from the National Science Foundation (CMMI-1130358) and the Laboratory Directed Research and Development program at Sandia National Laboratories. Sandia is a multiprogram laboratory operated by Sandia Corporation, a Lockheed Martin Company, for the United States Department of Energy under contract DE-ACO4-94AL85000.

References

- 1 B. K. Kim, S. Y. Lee and M. Xu, *Polymer*, 1996, **37**, 5781–5793.
- 2 A. Lendlein and S. Kelch, *Angewandte Chemie International Edition*, 2002, **41**, 2034–2057.
- 3 C. Liu, H. Qin and P. T. Mather, *Journal of Materials Chemistry*, 2007, **17**, 1543–1558.
- 4 C. M. Yakacki, R. Shandas, D. Safranski, A. M. Ortega, K. Sassaman and K. Gall, *Advanced Functional Materials*, 2008, **18**, 2428–2435.
- 5 M. Behl, M. Razzaq and A. Lendlein, *Advanced Materials*, 2010, **22**, 3388–3410.
- 6 C. M. Yakacki, A. M. Ortega, C. P. Frick, N. Lakhera, R. Xiao and T. D. Nguyen, *Macromolecular Materials and Engineering*, 2012, **297**, 1160–1166.
- 7 H. Luo, Y. Liu, Z. Yu, S. Zhang and B. Li, *Biomacromolecules*, 2008, **9**, 2573–2577.
- 8 A. Lendlein, H. Jiang, O. Junger and R. Langer, *Nature*, 2005, **434**, 879–882.
- 9 K. N. Long, T. F. Scott, H. J. Qi, C. N. Bowman and M. L. Dunn, *Journal of the Mechanics and Physics of Solids*, 2009, **57**, 1103–1121.
- 10 L. Wu, C. Jin and X. Sun, *Biomacromolecules*, 2010, **12**, 235–241.
- 11 S.-Q. Wang, D. Kaneko, M. Okajima, K. Yasaki, S. Tateyama and T. Kaneko, *Angewandte Chemie International Edition*, 2013, **52**, 11143–11148.
- 12 X.-J. Han, Z.-Q. Dong, M.-M. Fan, Y. Liu, Y.-F. Wang, Q.-J. Yuan, B.-J. Li and S. Zhang, *Macromolecular Rapid Communications*, 2012, **33**, 1055–1060.
- 13 B. Yang, W. Huang, C. Li, C. Lee and L. Li, *Smart Materials and Structures*, 2004, **13**, 191–195.
- 14 W. Huang, B. Yang, L. An, C. Li and Y. Chan, *Applied Physics Letters*, 2005, **86**, 114105.
- 15 S. Chen, J. Hu, C. Yuen and L. Chan, *Polymer*, 2009, **50**, 4424–4428.
- 16 H. Du and J. Zhang, *Soft Matter*, 2010, **6**, 3370–3376.
- 17 X. Gu and P. T. Mather, *Rsc Advances*, 2013, **3**, 15783–15791.
- 18 H. Lu, Y. Liu, J. Leng and S. Du, *European Polymer Journal*, 2010, **46**, 1908–1914.
- 19 C. C. Wang, Y. Zhao, H. Purnawali, W. M. Huang and L. Sun, *Reactive and Functional Polymers*, 2012, **72**, 757–764.

-
- 20 Z.-Q. Dong, Y. Cao, Q.-J. Yuan, Y.-F. Wang, J.-H. Li, B.-J. Li and S. Zhang, *Macromolecular Rapid Communications*, 2013, **34**, 867–872.
- 21 J. Zhang, W. Huang, H. Lu and L. Sun, *Materials & Design*, 2014, **53**, 1077–1088.
- 22 P. T. Mather, X. Luo and I. Rousseau, *Annual Review of Materials Research*, 2009, **39**, 445–471.
- 23 M. Behl, U. Ridder, Y. Feng, S. Kelch and A. Lendlein, *Soft Matter*, 2009, **5**, 676–684.
- 24 M. Behl, I. Bellin, S. Kelch, W. Wagermaier and A. Lendlein, *Advanced Functional Materials*, 2009, **19**, 102–108.
- 25 M.-M. Fan, Z.-J. Yu, H.-Y. Luo, S. Zhang and B.-j. Li, *Macromolecular Rapid Communications*, 2009, **30**, 897–903.
- 26 S. Zhang, Z. Yu, T. Govender, H. Luo and B. Li, *Polymer*, 2008, **49**, 3205–3210.
- 27 S. Alexander, R. Xiao and T. D. Nguyen, *Journal of Applied Mechanics*, 2014, **81**, 041003.
- 28 D. P. Nair, N. B. Cramer, T. F. Scott, C. N. Bowman and R. Shandas, *Polymer*, 2010, **51**, 4383–4389.
- 29 S. Chatani, C. Wang, M. Podgórski and C. N. Bowman, *Macromolecules*, 2014, **47**, 4949–4954.
- 30 W. Wagermaier, K. Kratz, M. Heuchel and A. Lendlein, *Shape-Memory Polymers*, Springer, 2010, pp. 97–145.
- 31 T. Xie, *Polymer*, 2011, **52**, 4985–5000.
- 32 G. J. Berg, M. K. McBride, C. Wang and C. N. Bowman, *Polymer*, 2014, **55**, 5849–5872.
- 33 T. D. Nguyen, *Polymer Reviews*, 2013, **53**, 130–152.
- 34 K. Yu, Q. Ge and H. J. Qi, *Nature Communications*, 2014, **5**, 1–9.
- 35 M.-C. Chen, H.-W. Tsai, Y. Chang, W.-Y. Lai, F.-L. Mi, C.-T. Liu, H.-S. Wong and H.-W. Sung, *Biomacromolecules*, 2007, **8**, 2774–2780.
- 36 W. Huang, *Open Medical Devices Journal*, 2010, **2**, 11–19.
- 37 W. Huang, C. Song, Y. Fu, C. Wang, Y. Zhao, H. Purnawali, H. Lu, C. Tang, Z. Ding and J. Zhang, *Advanced Drug Delivery Reviews*, 2013, **65**, 515–535.
- 38 Y. Yuan, J. E. Goodson, M. H. Johnson, D. Gerrard *et al.*, *SPE Drilling & Completion*, 2012, **27**, 253–263.
- 39 R. Xiao, J. Choi, N. Lakhera, C. Yakacki, C. Frick and T. Nguyen, *Journal of the Mechanics and Physics of Solids*, 2013, **61**, 1612–1635.
- 40 B. Yang, W. Huang, C. Li and L. Li, *Polymer*, 2006, **47**, 1348–1356.
- 41 R. Xiao and T. D. Nguyen, *Soft Matter*, 2013, **9**, 9455–9464.
- 42 H. Lu, W. M. Huang, Y. Fu and J. Leng, *Smart Materials and Structures*, 2014, **23**, 125041.
- 43 P. Ping, W. Wang, X. Chen and X. Jing, *Biomacromolecules*, 2005, **6**, 587–592.
- 44 K. Gall, C. M. Yakacki, Y. Liu, R. S. adn N. Willet and K. S. Anseth, *Journal of Biomedical Materials Research: Part A*, 2005, **73**, 339–348.
- 45 Z. Wang, Z. Li, L. Wang., Z. Xiong, Z. Wang, Z. Li, L. Wang and Z. Xiong, *Journal of Applied Polymer Science*, 2010, **118**, 1406–1413.
- 46 G. Rabani, H. Luftmann and A. Kraft, *Polymer*, 2006, **47**, 4251–4260.
- 47 N. Lakhera, C. M. Yakacki, T. Nguyen, C. P. Frick *et al.*, *Journal of Applied Polymer Science*, 2012, **126**, 72–82.
- 48 S. Li and W. Huang, *Soft Matter*, 2010, **6**, 4403–4406.
- 49 T. Xie and K. A. Page, *Advanced Functional Materials*, 2011, **21**, 2057–2066.
- 50 K. Yu, T. Xie, J. Leng, Y. Ding and H. J. Qi, *Soft Matter*, 2012, **8**, 5687–5695.
- 51 M. Behl, K. Kratz, U. Noechel, T. Sauter and A. Lendlein, *Proceedings of the National Academy of Sciences*, 2013, **110**, 12555–12559.
- 52 K. Yu and H. J. Qi, *Soft Matter*, 2014, **10**, 9423–9432.
- 53 R. Xiao, J. Guo and T. D. Nguyen, *RSC Advances*, 2015, **5**, 416–423.
- 54 Y. Wang, J. Li, X. Li, Y. Pan, Z. Zheng, X. Ding and Y. Peng, *RSC Advances*, 2014, **4**, 20364–20370.
- 55 T. Xie, *Nature*, 2010, **464**, 267–270.
- 56 J. Li, T. Liu, S. Xia, Y. Pan, Z. Zheng, X. Ding and Y. Peng, *Journal of Materials Chemistry*, 2011, **21**, 12213–12217.
- 57 J. Li, T. Liu, Y. Pan, S. Xia, Z. Zheng, X. Ding and Y. Peng, *Macromolecular Chemistry and Physics*, 2012, **213**, 2246–2252.
- 58 Y. Zhao, C. C. Wang, W. M. Huang and H. Purnawali, *Applied Physics Letters*, 2011, **99**, 131911.
- 59 J. L. Zhang, W. M. Huang, G. Gao, J. Fu, Y. Zhou, A. V. Salvekar, S. S. Venkatraman, Y. S. Wong, K. H. Tay and W. R. Birch, *European Polymer Journal*, 2014, **58**, 41–51.
- 60 W. M. Huang, H. B. Lu, Y. Zhao, Z. Ding, C. C. Wang, J. L. Zhang, L. Sun, J. Fu and X. Y. Gao, *Materials & Design*, 2014, **59**, 176–192.
- 61 F. Grillard, C. Zakri, P. Gaillard, A. Korzhenko, W. Néri and P. Poulin, *Soft Matter*, 2014, **10**, 8985–8991.
- 62 P. Miaudet, A. Derre, M. Maugey, C. Zakri, P. M. Piccione, R. Inoubli and P. Poulin, *Science*, 2007, **318**, 1294–1296.
- 63 R. S. Yeo, *Polymer*, 1980, **21**, 432–435.
- 64 R. Yeo and C.-H. Cheng, *Journal of Applied Polymer Science*, 1986, **32**, 5733–5741.
- 65 G. Gebel, P. Aldebert and M. Pineri, *Polymer*, 1993, **34**, 333–339.
- 66 S. K. Young, S. Trevino and N. C. Beck Tan, *Journal of Polymer Science Part B: Polymer Physics*, 2002, **40**, 387–400.
- 67 A. Vishnyakov and A. V. Neimark, *The Journal of Physical Chemistry B*, 2000, **104**, 4471–4478.
- 68 A. Vishnyakov and A. V. Neimark, *The Journal of Physical Chemistry B*, 2001, **105**, 7830–7834.
- 69 G. Adam and J. H. Gibbs, *Journal of Chemical Physics*, 1965, **43**, 139–146.
- 70 E. Dimarzio and J. Gibbs, *Journal of Polymer Science Part A: General Papers*, 1963, **1**, 1417–1428.
- 71 T. Chow, *Macromolecules*, 1980, **13**, 362–364.
-